RESEARCH ARTICLE OPEN ACCESS

The Use of HYSPLIT Model to Determine the Affected Areas of Dispersed Sea-Salt Particles of Dried Urmia Lake

Mahshid Nasiri*, Khosro Ashrafi**, Fereydoun Ghazban***
*(Faculty of environment, Tehran University, Iran)
** (Faculty of environment, Tehran University, Iran)
*** (Faculty of environment, Tehran University, Iran)

ABSTRACT
Urmia Lake is one of the largest permanent hypersaline lakes in the world. In order to study the effects of aridity of Urmia Lake in northwestern Iran on local air quality, the Hybrid Single- Particle Lagrangian Integrated Trajectory (HYSPLIT) model is used to model the dispersion of remained sea-salt particles on the basin. Due to determine the possible affected areas at periphery of Urmia Lake and estimate the aerosol concentration in these areas, 24 hour dispersion has been modeled under various wind directions. Wind directions have been chosen regarded to prevailing wind in the area which is northeast-southwest. The maximum number of affected areas of sea-salt particles dispersion will be under 240 degree wind while the highest concentration of 6400 µg/m^3 will occur under 90 degree wind.

***Keywords* -** Urmia Lake, Sea-salt aerosols, HYSPLIT

I. INTRODUCTION

Lake Urmia in the northwestern Iran is one of the largest permanent hypersaline lakes in the world ([1], [2], [3]). The decline of lake's surface area is generally blamed on a combination of drought, increased water diversion for irrigated agriculture within the lake's watershed and mismanagement ([1], [2], [4], [5]). In addition, a causeway has been built across the lake with only a 1500 m gap for water to move between the northern and southern halves of the lake ([4]). It has been suggested that this has decreased circulation within the lake and altered the pattern of water chemistry; however evidence suggests that the impact of the causeway on the uniformity of water chemistry in the lake has been minimal ([4], [5], [6], [7]).

A study based on the modeling of the relative influence of various factors on the decline of Lake Urmia found that 65% of the decline was from changes in inflow caused by recent global climate change and diversion of surface water for upstream use, with the remaining balance due to construction of dams (25%) and decreased precipitation over the lake itself (10%) ([2]). As the lake levels decline, the exposed lakebed is left with a covering of salts, primarily sodium chloride, making a great salty desert (Figure1). These salt flats are detrimental to agriculture and inhibit growth of most natural vegetation. The salts are also susceptible to blowing and will likely create "salt-storms". Sea-salt aerosols, together with wind-blown mineral dust, and naturally occurring chloride and organic compounds, are part of natural tropospheric aerosols. Tropospheric aerosols are a concern to health, with consequences for the respiratory tract ([8]); moreover, they affect ecosystems by reducing photosynthetic activity, and manufactured items by contributing to corrosion ([9]). Aerosols also represent a climate issue ([10]), because they modify radiative forcing, heat distribution within the atmosphere (and thus atmospheric circulation), and cloud formation and as a result hydrological cycle ([11]). People around the lake fear a fate similar to that of the population surrounding the nearby Aral Sea, which dried up over the past several decades. Disappearance of the Aral Sea has been an environmental disaster affecting people throughout the region with windblown salt-storms. The population surrounding Lake Urmia is much denser setting more people at risk of impact. The objective of this study was to estimate the effect of aridity of Lake Urmia on local air quality. Many different dust storm models have been developed to study regional and/or global dust storm properties ([12], [13], [14], [15], [16], [17], [18]). A new windblown dust emission algorithm was developed by Draxler et al. (2010) matching the frequency of high AOD events derived from the MODIS Deep Blue algorithm with the frequency of friction velocities derived from NCEP's North American Mesoscale (NAM) forecast model. The threshold friction velocity has been defined as the friction velocity that has the same frequency of occurrence as the 0.75-AOD which is derived from the result of a five-year climatology analysis of the MODIS AODs ([19]).

Urmia Lake is continuing to dry out and yet no detailed study has been carried out on the effects of its aridity on local air quality. Comparing the situations of Urmia Lake and Aral Sea (Figure2) and considering the AOD of Aral Sea (figure3) which is obtained from the NASA-operated GIOVANNI portal (http://disc.sci.gsfc.nasa.gov/giovanni), came to this conclusion that the AOD of Urmia Lake will reach 0.75 and the new algorithm ([20]) can be used for modeling the dispersion of sea salt aerosols of dried Urmia Lake. For this work, the last revision of the Hybrid Single-Particle Lagrangian Integrated Trajectory (HYSPLIT) model ([21]) has been used.

Fig.1. Satellite image showing the entire Lake Urmia with the Exposed lakebed in the shore line and also around the islands in the southern part of the lake covered by salt

Fig.2. (a) Urmia Lake (b) Aral Sea

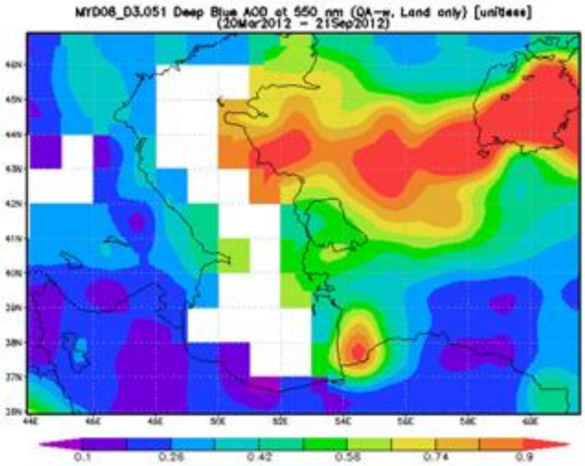

Fig.3. Terra MODIS satellite image shows the difference between deep blue AOD of Urmia Lake and Aral Sea. The increase of AOD suggests the higher possibility of dust storm occurrence

II. Materials and Methods

2.1. Meteorological data

In order to determine the effects of meteorological parameters on sea-salt particle concentration, the dispersion of aerosols has been modeled under constant wind speed. The wind speed distribution of 2010 in Tabriz and Urmia, as two major cities at periphery of the Lake has been shown in table 1 and table 2.The prevailing wind at periphery of the Lake is northeast-southwest and based on the data mentioned in tables 1 and 2, the wind speeds of 1-3 m/s have the most frequency.

Tab. 1. Wind speed distribution in Tabriz

	Wind Speed Distribution (hours)									Fastest Wind		
Month	1 to 3 m/s	4 to 6 m/s	7 to 10 m/s	11 to 16 m/s	17 to 21 m/s	22 to 27 m/s	28 to 33 m/s	34 to 42 m/s	42 more	Direction	Speed	day
January	161	43	16	6	0	0	0	0	0	220	20	4
February	157	36	11	2	0	0	0	0	0	240	20	22
March	108	79	32	15	0	0	0	0	0	230	22	31
April	122	74	18	7	0	0	0	0	0	240	16	13
May	126	79	28	2	0	0	0	0	0	250	18	15
June	106	85	36	5	0	0	0	0	0	360	17	20
July	65	109	67	3	0	0	0	0	0	50	14	20
August	87	99	51	2	0	0	0	0	0	320	16	26
September	125	75	30	0	0	0	0	0	0	350	17	23
October	156	56	23	1	0	0	0	0	0	220	18	10
November	199	23	0	0	0	0	0	0	0	260	6	9
December	181	44	2	0	0	0	0	0	0	260	13	13
Year	1593	802	314	43	0	0	0	0	0	230	22	31

Tab. 1. Wind speed distribution in Urmia

	Wind Speed Distribution (hours)									Fastest Wind		
Month	1 to 3 m/s	4 to 6 m/s	7 to 10 m/s	11 to 16 m/s	17 to 21 m/s	22 to 27 m/s	28 to 33 m/s	34 to 42 m/s	42 more	Direction	Speed	day
January	178	24	7	2	0	0	0	0	0	230	13	4
February	172	23	4	0	0	0	0	0	0	210	9	16
March	160	45	15	7	0	0	0	0	0	180	18	15
April	163	48	8	1	0	0	0	0	0	250	13	13
May	194	38	5	1	0	0	0	0	0	230	12	23
June	188	39	4	1	0	0	0	0	0	270	12	15
July	189	46	2	0	0	0	0	0	0	350	7	17
August	195	40	0	0	0	0	0	0	0	270	12	26
September	192	37	2	0	0	0	0	0	0	240	10	14
October	180	49	8	0	0	0	0	0	0	250	11	2
November	204	9	0	0	0	0	0	0	0	60	5	1
December	215	12	1	0	0	0	0	0	0	240	8	18
Year	2230	410	45	12	0	0	0	0	0	180	18	15

2.2. HYSPLIT Model

The HYSPLIT model is a complete system for computing trajectories, complex dispersion, and deposition simulations using either puff or particle

Approaches ([21]). The model was first applied to simulate desert sand and dust storms to estimate PM_{10} concentrations in Iraq, Kuwait and Saudi Arabia ([22]). Subsequently, a more generalized and simple dust emission formulation was incorporated into HYSPLIT for application to regions without detailed digital soil characteristics and was tested in the North African regions ([23]). Recently, the HYSPLIT dust model has been improved for application over the Western United States with a new empirically derived approach based on MODIS (Moderate Resolution Imaging Spectroradiometer) AOD (Aerosol Optical Depth) values ([20]). The module for the emission of PM_{10} dust has been constructed using the concept of a threshold friction velocity which is dependent on surface roughness. Surface roughness was correlated with geomorphology or soil properties and a dust emission rate is computed where the local wind velocity exceeds the threshold velocity for the soil characteristics of that emission cell ([20]; [24])

$$q = K\, f(u_*) \quad (1)$$

$$f(u_*) = u_* - u_{*t} \quad (2)$$

To use the relationship between u_* and K in a model simulation, the emission flux (Eq. 1) must be converted to the mass emitted over a grid cell by multiplying the flux by the area of each grid cell covered by dust sources (A_d), so a grid cell's total emission rate would be:

$Q = q\ A_d$ (3)

The total catchment area of the lake is about 51,876 Km^2 which is 3.15% of that of the entire country, and includes 7% of the total surface water in Iran. In order to consider the whole area of lake as the source, area is adjusted with each point so that the total area over all points represents the area of the lake. Lake Urmia, is one of the largest permanent hyper-saline lakes in the world and resembles the Great Salt Lake in the western USA in many respects of morphology, chemistry and sediments ([25]). Because of the similarity between Urmia Lake and Great Salt Lake, the dust density of soil as defined K, is considered to be 6.0E-04 ([20]).

III. Results and discussion

3.1 Threshold friction velocity

Threshold friction velocity u_{*t} represents the capacity of an aeolian surface to resist wind erosion. At $u_* = u_{*t}$ the aerodynamic forces just overcome the retarding forces and initialize the movement of soil particles. In reality, u_{*t} is affected by a range of factors such as soil texture, soil moisture, soil salt content, surface crust, the distribution of vegetation, and roughness elements. Under ideal conditions, u_{*t} can be expressed as a function of only particle size. Several theories for $u_{*t}(d)$ exist, derived for soils with uniform and spherical particles spread loosely over a dry and bare surface ([26], [27], [28]). In this study an expression for calculating the wind erosion threshold friction velocity u_{*t} for spherical particles loosely spread over a dry and bare surface was used. This expression takes into account the effect of inter particle cohesion on u_{*t} but retains a simple functional form ([29]):

$$u_{*t} = [\ A_N(\sigma_p\ g\ d + \gamma/\rho d)]^{0.5} \qquad (4)$$

With A_N being around 0.0123 and γ being around 3×10^{-4} Kgs^{-2}. The key argument embedded in the new expression is that the inter particle cohesive force should be, in general, proportional to d^{-1}. For d< 50 µm, the cohesive force is at least 100 times larger than the gravity force ([29]). So for PM_{10} (particle with diameter of 10 µm and less), the threshold friction velocity will decrease with increasing the diameter of particle. In this study, in order to consider the critical situation to predict the emission of sea salt particles, the diameter of 10µm was considered for dry sea salt particles with density of 2.17 gcm^{-3}.

3.2. Aerosol concentration

The Model was run in order to portray the changes of average concentration of sea-salt particles under various wind speeds. Due to determine the effect of wind direction on aerosol concentration, the wind speed of 3 m/s has been considered constant. Figure 4 shows the daily average concentration under various wind directions. The directions have been chosen regarded to prevailing wind in the area.

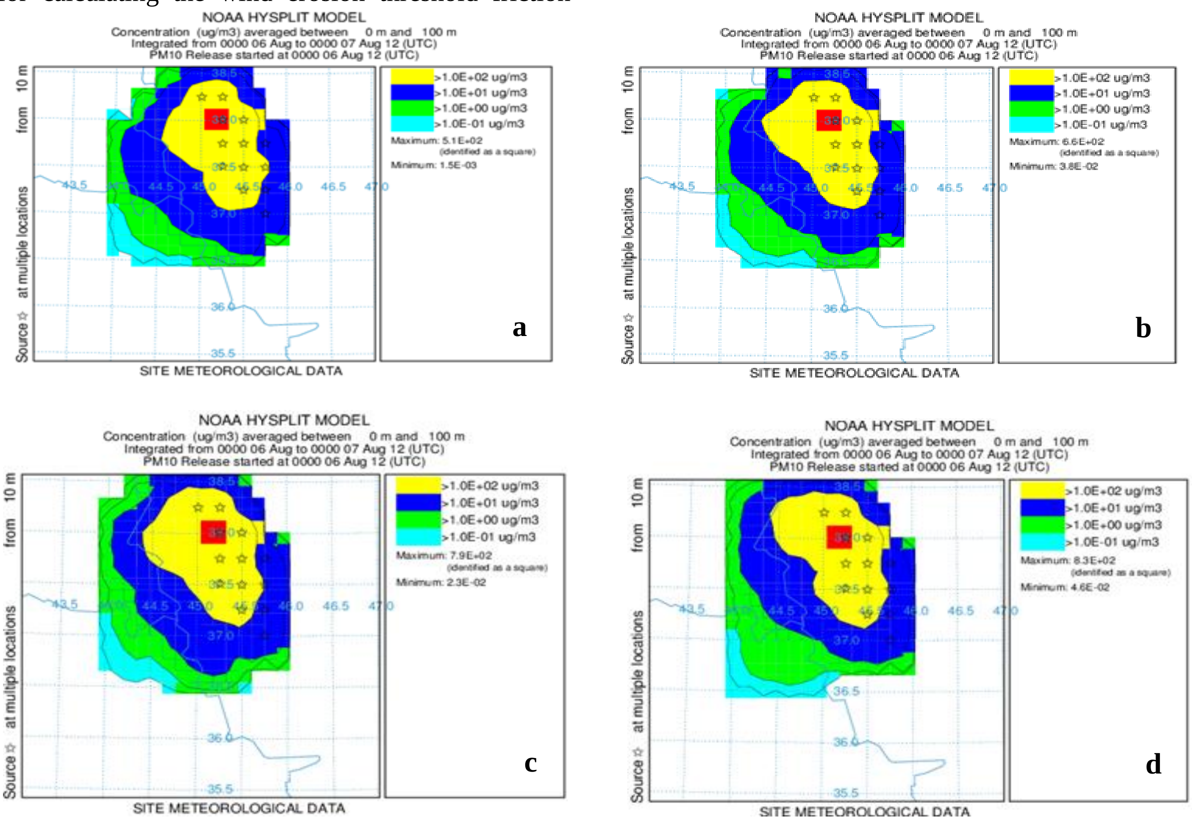

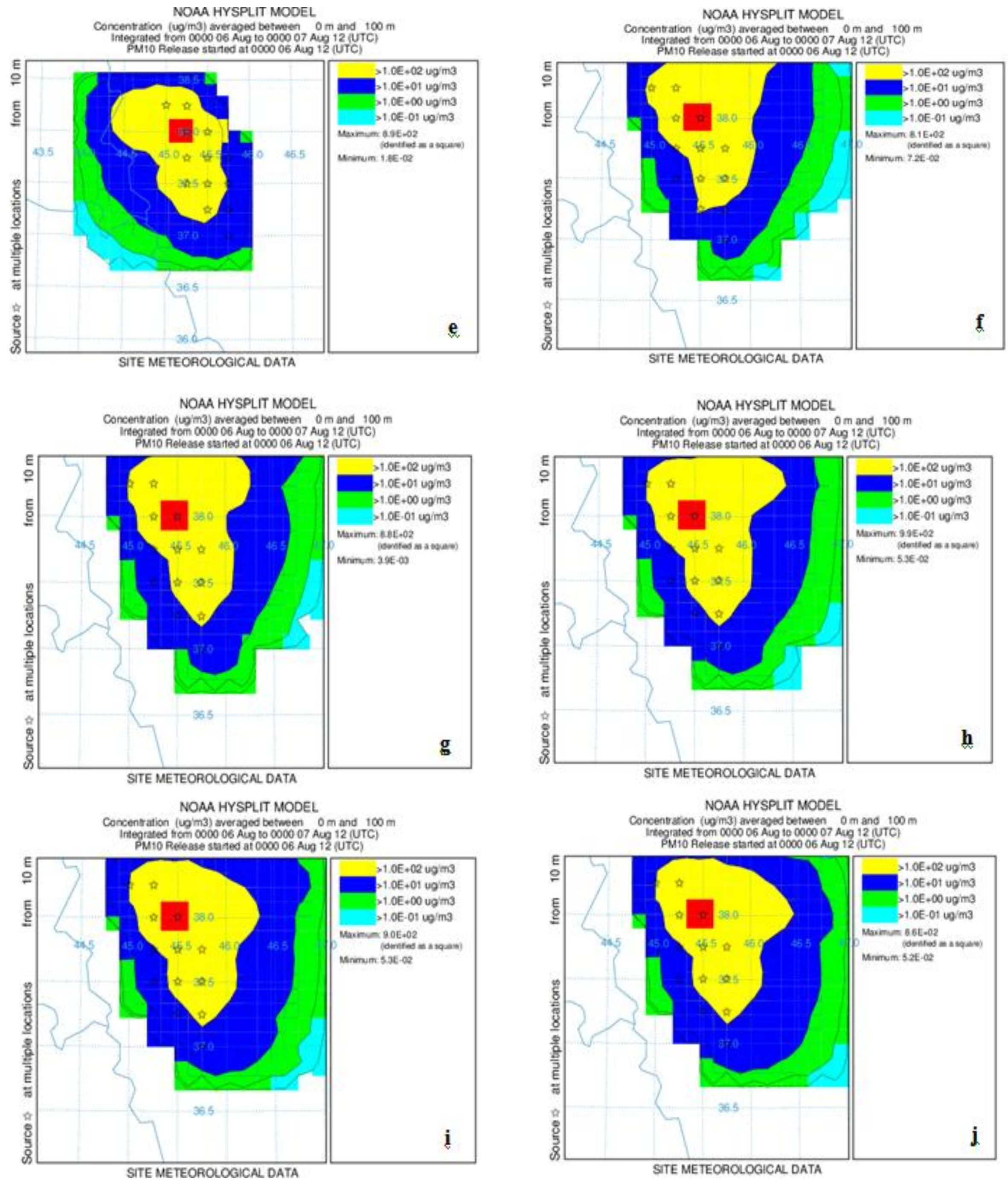

Fig.4.sea-salt dispersion under various wind direction (a)50˚ (b)60˚ (c)70˚ (d)80˚ (e)90˚ (f)230˚ (g)240˚ (h)250˚ (i) 260˚ (j)270˚

The model has been run to determine the 24 hour average concentration under different speed directions (50˚, 60˚, 70˚, 80˚, 90˚, 230˚, 240˚, 250˚, 260˚, 270˚).Figure 4 shows concentrations for each run. The concentration for each location which has been affected during 24 hour dispersion has been shown in figure 5.

Based on the result, although the highest concentration will occur under 90 degree wind which will be 6400 µg/m^3, but 60 degree and 240 degree winds will affect maximum number of locations. The highest concentration under 60 degree wind will be 4900 µg/m^3 in 37.95N, 45.15E and the highest concentration under 240 degree wind will be 5100 µg/m^3 in 38.05N, 45.35E.

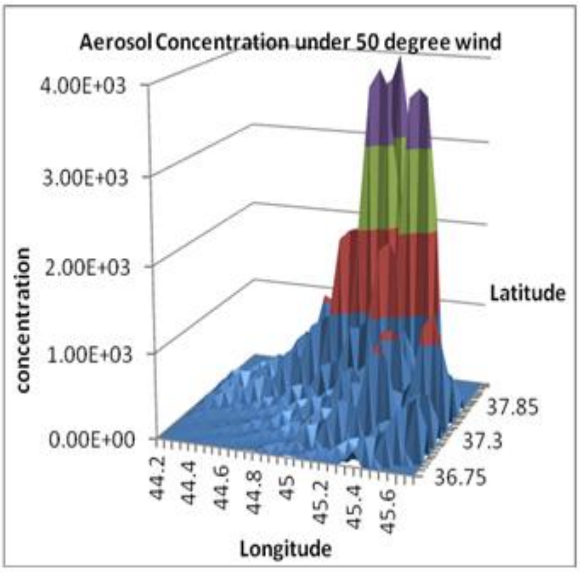
Aerosol Concentration under 50 degree wind
4.00E+03
3.00E+03
2.00E+03
1.00E+03
0.00E+00
concentration
Latitude
37.85
37.3
36.75
44.2
44.4
44.6
44.8
45
45.2
45.4
45.6
Longitude

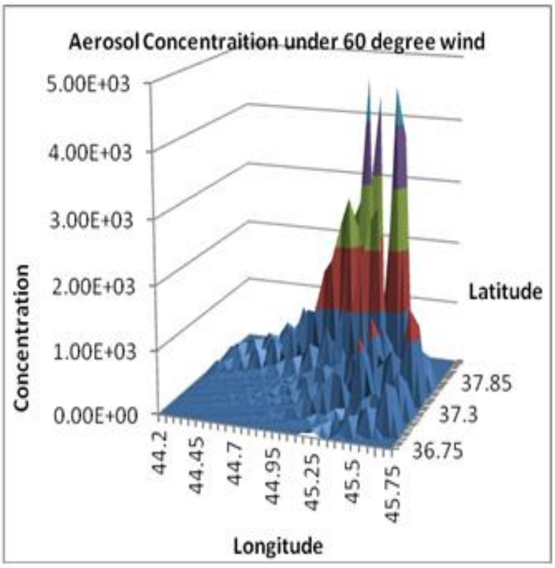
Aerosol Concentraition under 60 degree wind
5.00E+03
4.00E+03
3.00E+03
2.00E+03
1.00E+03
0.00E+00
Concentration
Latitude
37.85
37.3
36.75
44.2
44.45
44.7
44.95
45.25
45.5
45.75
Longitude

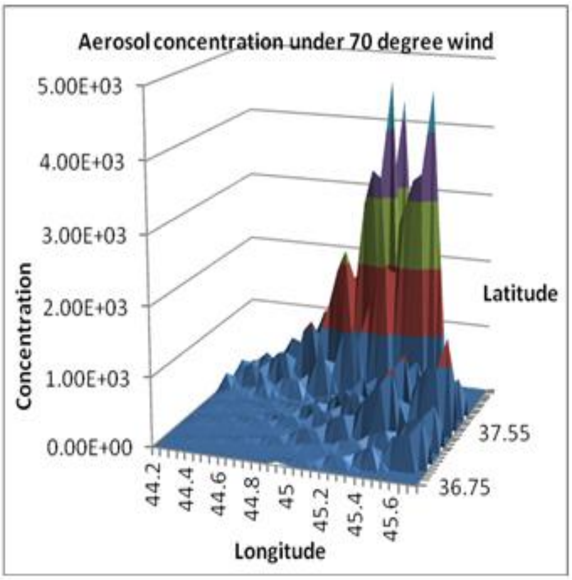
Aerosol concentration under 70 degree wind
5.00E+03
4.00E+03
3.00E+03
2.00E+03
1.00E+03
0.00E+00
Concentration
Latitude
37.55
36.75
44.2
44.4
44.6
44.8
45
45.2
45.4
45.6
Longitude

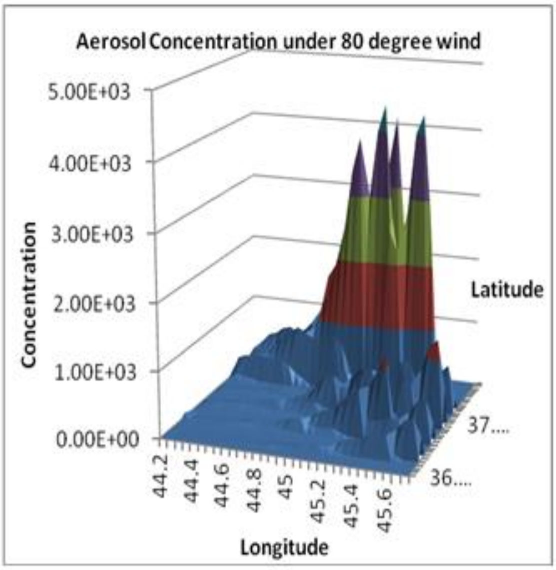
Aerosol Concentration under 80 degree wind
5.00E+03
4.00E+03
3.00E+03
2.00E+03
1.00E+03
0.00E+00
Concentration
Latitude
37....
36....
44.2
44.4
44.6
44.8
45
45.2
45.4
45.6
Longitude

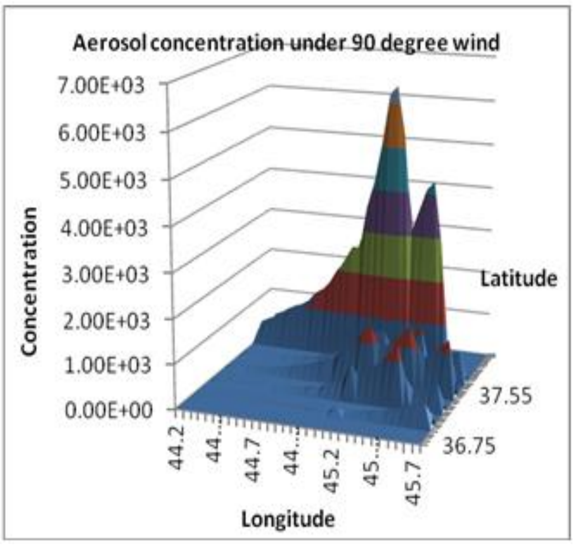
Aerosol concentration under 90 degree wind
7.00E+03
6.00E+03
5.00E+03
4.00E+03
3.00E+03
2.00E+03
1.00E+03
0.00E+00
Concentration
Latitude
37.55
36.75
44.2
44....
44.7
44....
45.2
45....
45.7
Longitude

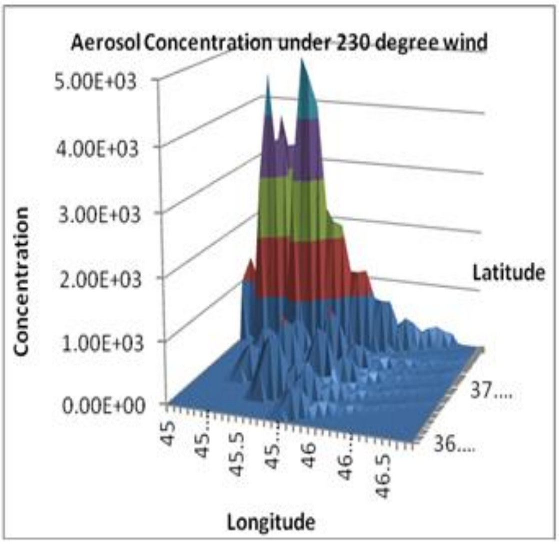
Aerosol Concentration under 230 degree wind
5.00E+03
4.00E+03
3.00E+03
2.00E+03
1.00E+03
0.00E+00
Concentration
Latitude
37....
36....
45
45....
45.5
45....
46
46....
46.5
Longitude

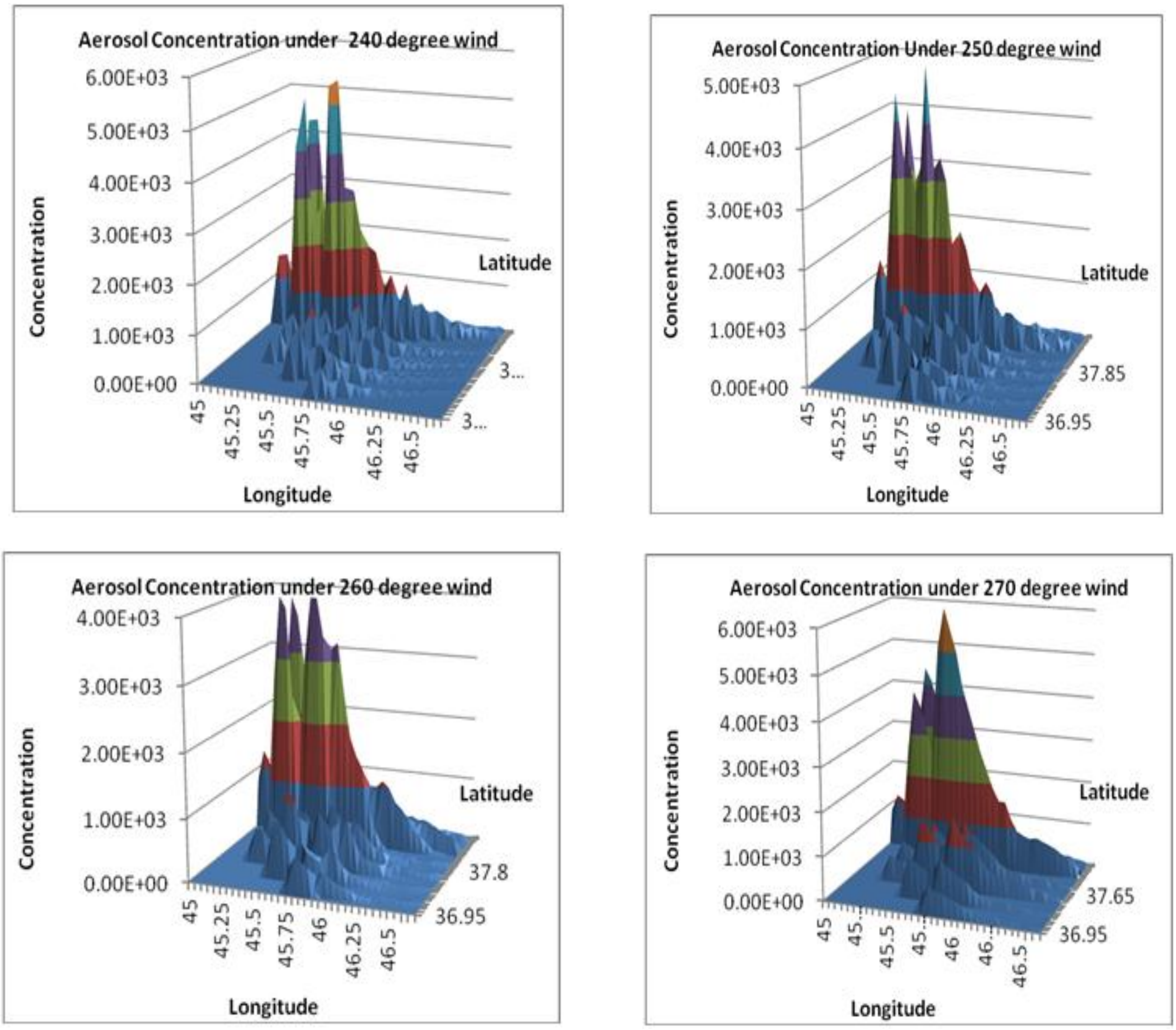

Fig.5. Concentration at affected areas under various wind direction

IV. Conclusion

The aridity of Urmia Lake as one of the largest permanent hyper-saline lakes in world is a major environmental concern, especially in the matter of its effects on air quality. Comparing the current situation of Urmia Lake and the situation of Aral Sea suggests the possibility of reaching current AOD to higher values and occurrence of dust storms at periphery of Urmia Lake. In this study, HYSPLIT is used for modeling the dispersion of sea-salt aerosols of dried Urmia Lake and determine the possible affected locations under different wind directions. Base on the results,60 degree and 240 degree winds will affect the maximum number of locations in the vicinity of the lake.

References

[1] M. Zarghami, Effective watershed management; Case study of Urmia Lake, Iran. *Lake and Reservoir Management, 27(1),2011. 87-94.*

[2] E. Hassanzadeh, M. Zarghami, Y. Hassanzadeh, Determining the Main Factors in Declining the Urmia Lake Level by Using System Dynamics Modeling. *Water Resources Management, 26(1),2011, 129-145.*

[3] . Karbassi, G. Bidhendi, A. Pejman, M. Bidhendi, Environmental impacts of desalination on the ecology of Lake Urmia. *Journal of Great Lakes Research, 36(3), 2010, 419-424.*

[4] A. Eimanifar, F. Mohebbi, Urmia Lake (Northwest Iran): a brief review. *Saline Systems, 2007 3-5.*

[5] H. Golabian, Urumia Lake: Hydro-Ecological Stabilization and Permanence Macro-engineering Seawater in Unique Environments, *2010, 365-397. Berlin: Springer-Verlag.*

[6] M. Zeinoddini, M. Tofighi, F. Vafaee, Evaluation of dike-type causeway impacts on the flow and salinity regimes in Urmia

Lake, Iran. *Journal of Great Lakes Research, 35(1), 2009, 13-22.*

[7] S. Alipour, Hydrogeochemistry of seasonal variation of Urmia Salt Lake, Iran. *Saline Systems, 2006, 2- 9.*

[8] R. L. Maynard, C. V. Howard, *Particulate matter: properties and effects upon health* (Oxford: BIOS Scientific Publishers. 1999)

[9] H. B. Singh, *Composition, chemistry and climate of the atmosphere* (New York: John Wiley and Sons, 1995)

[10] J. T. Houghton, Y. Ding, D. J. Griggs, M. Noguer. P. J. van der Linden, X. Dai, *Climate change: the scientific basis* (Cambridge: Cambridge University Press, 2001)

[11] C. N. Cruz , S. N. Pandis, A study of the ability of pure secondary organic aerosol to act as cloud condensation nuclei. *Atmos Environ, 31, 1997, 2205–2214*

[12] P. Ginoux, M. Chin, I. Tegen, J. M. Prospero, B. Holben, O. Dubovik, S. J. Lin, Sources and distributions of dust aerosols simulated with the GOCART model. *Journal of Geophysical Research 106 (D17), 2001, 20255-20273*

[13] S. L. Gong, X. Y. Zhang, T. L. Zhao, I. G. Mckendry, D. A. Jaffe, N. M. Lu, Characterization of soil dust aerosol in China and its transport/distribution during 2001 ACE-Asia, 2. Model simulation and validation. *Journal of Geophysical Research 108 (D9), 2003, 4262-4270*

[14] C. Pérez, S. Nickovic, J. M. Baldasano, M. Sicard, F. Rocadenbosch, A long Saharan dust event over the western Mediterranean: lidar, sun photometer observations, and regional dust modeling. *Journal of Geophysical Research 111, D15214, 2006*

[15] Y. Shao, A model for mineral dust emission. *Journal of Geophysical Research 106 (D17), 2001, 20239-20254.*

[16] I. Uno, H. Amano, S. Emori, K. Kinoshita, I. Matsui, N. Sugimoto, Trans-Pacific yellow sand transport observed in April 1998: a numerical simulation. *Journal of Geophysical Research 106 (D16), 2001, 18331-18344.*

[17] C. S. Zender, H. Bian, D. Newman, Mineral dust entrainment and deposition (DEAD) model: description and 1990's dust climatology. *Journal of Geophysical Research 108 (D14), 2003*

[18] C. H. Zhou, S. I. Gong, X. Y. Zhang, Y. Q. Wang, T. Niu, H. I. Liu, T. L. Zhao, Y. Q. Yang, Q. Hou, Development and evaluation of an operational SDS forecasting system for East Asia: CUACE/dust. *Atmospheric Chemistry and Physics 8, 2008, 787-798.*

[19] P. Ginoux, D. Garbuzov, N. C. Hsu, Identification of anthropogenic and natural dust sources using MODIS Deep Blue level 2 data. *Journal of Geophysical Research 115, D05204, 2010*

[20] R. R. Draxler. P. Ginoux. A. F. Stein, An empirically derived emission algorithm for windblown dust, *Journal of Geophysical Research, 115, D16212, 2010*

[21] R. R. Draxler, G. D. Hess, An overview of the HYSPLIT_4 modeling system for trajectories, dispersion, and deposition. *Australian Meteorological Magazine 47, 1998, 295-308.*

[22] R. R. Draxler, D. A. Gillete, J. S. Kirkpatrick, J. Heller, Estimating PM10 air concentrations from dust storms in Iraq, Kuwait and Saudi Arabia. *Atmospheric Environment 35, 2001, 4315-4330.*

[23] M. Escudero, A. Stein, R. R. Draxler, X. Querol, A. Alastuey, S. Castillo, A. Avila, Determination of the contribution of northern Africa dust source areas to PM10 concentrations over the central Iberian Peninsula using the hybrid single-particle Lagrangian Integrated Trajectory model (HYSPLIT) model. *Journal of Geophysical Research 111, D06210, 2006.*

[24] Y. Wang. A. F. Stein, R. R. Draxler, J. D. de la Rosa, X. Zhang. Global sand and dust storms in 2008: Observation and HYSPLIT model verification, *Atmospheric Environment ,45, 2011, 6368-6381*

[25] K. Kelts. M. Shahrabi. Holocene sedimentalogy of hyper-saline Lake Urmia, northwestern Iran. *Paleogeography, Paleoclimatology and Paleoecology, 54, 1986, 105-130*

[26] R. A. Bagnold, 1941. *The Physics of Blown Sand and Desert Dunes* (Methuen, New York, 1941)

[27] R. Greeley, J. D. Iversen, *Wind as a Geological Process on Earth, Mars, Venus and Titan*, (Cambridge Univ. Press, New York, 1985)

[28] M. Phillips, A force balance model for particle entrainment into a fluid stream, *J. Phys. D Appl. Phys., 13, 1980, 221-233*

[29] Y. Shao. H. Lu, A simple expression for wind erosion threshold friction velocity, *Journal of Geophysical Research, Vol. 105, No. D17, 2000, 22,437-22,443*